2013

Synthesis of DNA-base selective labels for efficient labeling of DNA for TEM Imaging

Rakesh Kumar
The University of Montana

Synthesis of DNA-base selective labels for efficient labeling of DNA for TEM Imaging

By

Rakesh Kumar

M. Sc Chemistry (Inorganic), University of Delhi, 2002
MS Interdisciplinary Studies, The University of Montana, 2009

Presented in partial fulfillment of the requirements
for the degree of

MA
In Chemistry, Inorganic

The University of Montana
Missoula, MT

Fall 2013

Approved by:

Prof. J. B. Alexander Ross, Dean of Graduate School

Prof. Edward Rosenberg (Chairperson)
Department of Chemistry and Biochemistry

Abstract

The goal of this project was to explore the possibility of high throughput DNA sequencing using high-resolution electron microscopy. This approach was recently made feasible by development of a DNA threading technique that allows the imaging of straight, single stranded DNA; and by the development of atom-by-atom analysis with Transmission Electron Microscopy (TEM). In an attempt to better understand the types of interactions that can occur between water-soluble versions of complex and DNA we have synthesized the series of single metal and tetrametallic compounds. In order to demonstrate proof of concept for the technique of visualizing metal complex bound on DNA with TEM we studied the reaction of the complexes $[Pt(en)Cl(NH_2R)]^+NO_3^-$ (en = ethylene diamine, Pt, Z = 78) with dGMP. We report here the successful visualization of the Pt atoms in the complex $[Pt(en)Cl(NH_2R)]^+NO_3^-$ (R= $C_8H_9NO_2$ (benzo[*d*][1,3]dioxol-5ylmethanamine, also known as piperonylamine) bound to DNA by TEM as well as kinetic study of a series of related complexes reacting with dGMP. The synthesis and dGMP binding of a Pt-triosmium conjugate is also reported.

ACKNOWLEDGEMENTS

First and foremost I would like to express my sincerest gratitude to Prof. Edward Rosenberg. He has provided me with guidance, support and knowledge throughout my research career at UM. For Prof. Rosenberg I have the utmost respect and will strive to represent the Rosenberg group to the best of my ability through out my professional career. My time in Rosenberg group has been enjoyable, educational and fulfilling. I would like to especially thank Mark Hughes, Vardharajan Kailasam, Jesse Allen, Ayesha Sharmin, Glenn Pinson and Geoffery abbott for their time and effort extended during my stay in the group. My sincere thanks also goes to Dr. Earle Adam for giving me hands on experience on instruments that I used through out the program. I owe much gratitude to the entire chemistry department and my committee members, for their encouragement. The staff of the department, the library and FSSS needs a special mention - their cooperation and timely help takes us all a long way. I gratefully acknowledge National Science Foundation (Grant No. CHE-1049567), Halcyon Molecular and The University of Montana for support of this research.

I am eternally indebted to my parents, elder brothers, elder sister and brother-in-law who have always supported me and encouraged me with their best wishes and constant backup. Without you, I would not be able to reach to the point where I am today. I will always work hard to make you proud and I will always strive to bring happiness to your lives. Last but not least I would like to thank my lovely wife Dr. Baby Pallavi, she was always there and stood by me through thick and thin.

TABLE OF CONTENTS

LIST OF FIGURES

LIST OF SCHEMES

LIST OF TABLES

LIST OF ABBREVIATIONS

A	Adenine
C	Cytosine
DMSO	Dimethyl Sulfoxide
dsDNA	Double stranded DNA
ssDNA	Single stranded DNA
G	Guanine
HRTEM	High Resolution Transmission Electron Microscopy
IR	Infrared
NMR	Nuclear Magnetic Resonance Spectroscopy
Os-bipy	Osmium tetroxide 2,2'-bipyridine
T	Thymine
TEM	Transmission Electron Microscopy
THF	Tetrahydrofuran
TMAO	Trimethyl amine N-oxide
Z	Atomic Number

1.1. Synthesis of DNA-base selective labels for efficient labeling of DNA for TEM Imaging

Knowledge of DNA sequences has become indispensable for basic biological research, and in numerous applied fields such as diagnostic, biotechnology, forensic biology, and biological systematic. Genetic information has provided hope of resolving some of the worst diseases plaguing mankind. However, this promise is waiting for cheaper, faster, and more accurate means of DNA sequencing. High-throughput sequencing technologies are intended to lower the cost of DNA sequencing beyond what is possible with standard dye-terminator methods.[1] Another method being used is nanopore sequencing where voltage (potential) applied when the nanopore is immersed in a conducting fluid.[2] Due to which slight electric current observed when conduction of ions occurs through nanopore. When single bases or strands of DNA pass through the nanopore the process can create a change in the magnitude of the current through the nanopore.

However, these methods suffer from short read lengths, high cost and insufficient throughput. DNA sequencing by electron microscopy has also been explored.

The first serious work on sequencing by electron microscopy was started in 1960's by Beer and Moudrianakis.[3-8] Later Whiting and Ottensmeyer also attempted to visualize labeled DNA strand to get sequence information.[9, 10]

However, it has never been successfully used to generate meaningful sequence information.

A new technology has been developed by Halcyon Molecular, Inc. called "molecular threading."[11, 12]

This technology is a surface independent tip-based method for stretching and depositing single-stranded DNA molecules. Further, the TEM approach provides direct visualization of the sequence of DNA molecules labeled by heavy metal (atomic number, Z > 70). The transmission electron microscopy (TEM) works by sending an electron beam through sample and onto a detector screen. Heavy metals in the sample impede or deflect the beam so that the electrons

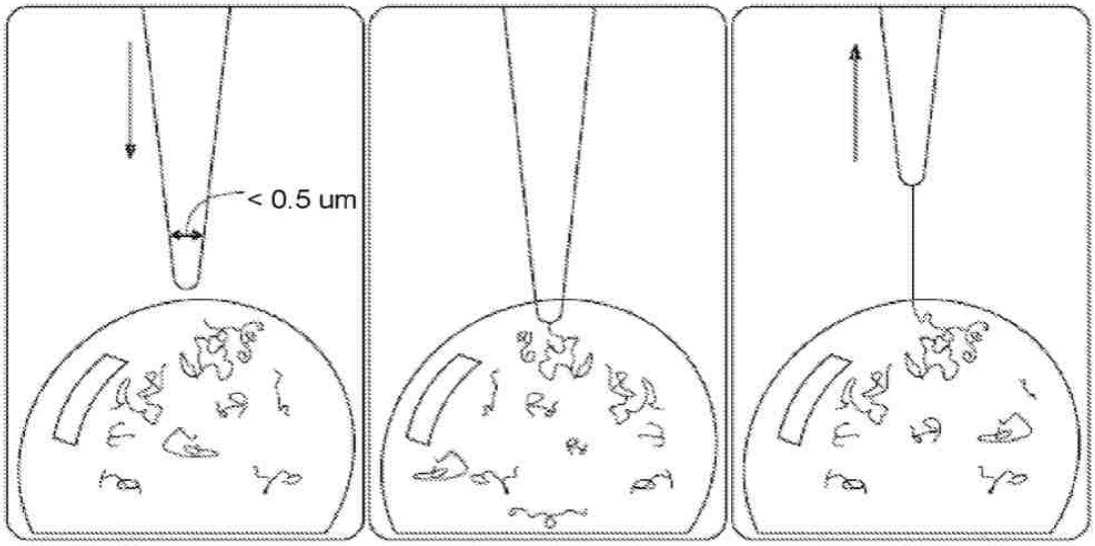

Figure. 1.1 Pictorial representation of molecular threading technique developed by Halcyon Molecular inc. where single stranded DNA is being pulled out straight before being placed on a support substrate or an imaging substrate.[11]

reaching the detector form an image. Atoms of low atomic number produce very little contrast and are essentially invisible in the electron microscope. Therefore DNA, comprising of low Z elements-carbon, hydrogen, nitrogen, oxygen, and phosphorus- shows almost no contrast against the supporting background in an electron microscope and, hence, is almost impossible to see. Hence visualization of DNA using current techniques in electron microscopy requires that the bases be labeled with high Z atoms.[13]

In the newly developed threading technique, DNA is stretched into air at a liquid-air interface and be subsequently deposited onto a dry substrate isolated from solution. Molecular threading demonstrates high degree of "straightness" and uniformity over length scales from nanometers to micrometers and represents a superior alternative to existing DNA deposition and linearization methods. Molecular threading, which includes both stretching and deposition, ensures that the base-to-base linear distance is uniform, which is an extremely important factor that lays the foundation for determining the DNA sequence by electron microscopy. This method allow controllable placement of nucleic acid on a substrate with consistent base-to-base spacing. Heavy-atom labeled nucleic acid polymers are imaged by electron microscopy to determine the position of the label along the polymer. A detector captures the images and positions of the label are recorded in a computer readable format. Pattern recognition software is then employed to use the spacing information to determine the base sequence information from the nucleic acid polymer. DNA sequence information obtained from a single strand is sufficient to derive the sequence of the complementary strand, which provides additional statistical support for the validity of a given base determination.

Although there are many advantages in using HRTEM the biggest disadvantage is the price-tag of the equipment and its running/maintenance expense. When the techniques of molecular threading and high-resolution TEM, with an imaging rate of about 500,000 bases per second, are used in conjunction the ultra-high throughput DNA sequencing seems achievable.

These results point towards scalable and high-throughput precision manipulation of single-stranded DNA.[12] Further, by using low cost TEM system will bring the cost down. The complete system is expected to read a complete haploid of human genome in days, perhaps hours. The goal to achieve the $1000 or less genome will then be possible.

The other requirement of this project is the ability to label the individual bases specifically with heavy atoms. The inherent drawback in using metal salts' staining is the lack of specificity to a nucleotide base owing to non-specific interactions. Therefore, covalent adduct formation between a DNA base and a metal complex is necessary for determination of the position of a specific base in a DNA molecule, thus, functionalized heavy metal complexes capable of base-specific labeling of DNA can provide a tool for DNA sequencing. Furthermore, the labels need to have high reactivity to attach themselves specifically to one of the four bases, GATC, along with very high specificity. We have been studying the interaction of benzoheterocycle complexes of triosmium carbonyl clusters for the last several years in our lab.[14-16]

Selectivity for guanine over the other bases was also observed.[15, 16]

In order to demonstrate proof of concept for the technique of visualizing a guanine bound metal complex on DNA with TEM we studied the reaction of the complexes $[Pt(en)Cl(NH_2R)]^+NO_3^-$ with dGMP and DNA. It was previously been shown that complexes of this type were selective for binding to guanine when R was a luminescent molecule.[17]

We report here the successful visualization of the Pt atoms in the complex $[Pt(en)Cl(NH_2R)]^+NO_3^-$ (R=$C_8H_9NO_2$(benzo[d][1,3]dioxol-5-ylmethanamine or piperonylamine) bound to DNA by TEM as well as qualitative kinetic study of a series of related complexes reacting with dGMP and the synthesis and dGMP binding of a Pt-triosmium conjugate.

Chapter 2: Synthesis of DNA-base selective labels for sequencing by TEM Imaging

2.1 Introduction

Beer and Moudrianakis (1962) first demonstrated that it might be possible to sequence DNA with the aid of the electron microscope.[3]

Transmission Electron Microscopy (TEM) has the potential to bring the base pair reading length up to 10^5 base-pairs per minute if the bases could be specifically labeled with heavy atoms. Long reading length enables detection of long repeating patterns in the genetic code and facilitates high-speed sequencing. Hence, the cost of DNA sequencing can be reduced significantly with the use of TEM. DNA has only light element (C,H,N,O,P), that are inherently transparent to TEM. Heavy metal ($Z > 70$) staining is well known to increase image contrast in TEM, and heavy metal salts have long been used in TEM to render nucleic acids visible.[3, 18-20] The relative number of electrons that are scattered to a detector is approximately proportional to $Z^{1.5}$. The inherent drawback in using metal salts' staining is the lack of specificity to a nucleotide base due to non-specific interactions. Therefore, covalent adduct formation between a DNA base and a metal complex is necessary for determination of the position of a specific base in a DNA molecule, Thus, functionalized heavy metal complexes capable of base-specific labeling of DNA can provide a tool for DNA sequencing. Furthermore, the labels need to have high reactivity to attach themselves specifically to one of the four bases, GATC, along with very high specificity. The key to getting sequence information from the heavy atom labeling is the ability to stretch a single strand of DNA onto a platform where multiple images of the strands can be added together

to give the exact sites of heavy atom labeling. Recently, such a technique has been developed, by Halcyon Molecular and provided the opportunity to develop heavy atom labels for DNA.[11]

We studied the reaction of the complexes $[Pt(en)Cl(NH_2R)]^+NO_3^-$ with dGMP and DNA in order to demonstrate proof of concept for the technique of visualizing a guanine bound metal complex on DNA with TEM. Similar complexes were previously been shown to be selective for binding to guanine where R was a luminescent molecule.[17]

In this chapter we reported the successful visualization of the Pt atoms in the complex $[Pt(en)Cl(NH_2R)]^+NO_3^-$ (R=$C_8H_9NO_2$ (benzo[*d*][1,3]dioxol-5-ylmethanamine, also known as piperonylamine) (**1**)) bound to DNA by TEM as well as a qualitative kinetic study of a series of related complexes reacting with dGMP.[21]

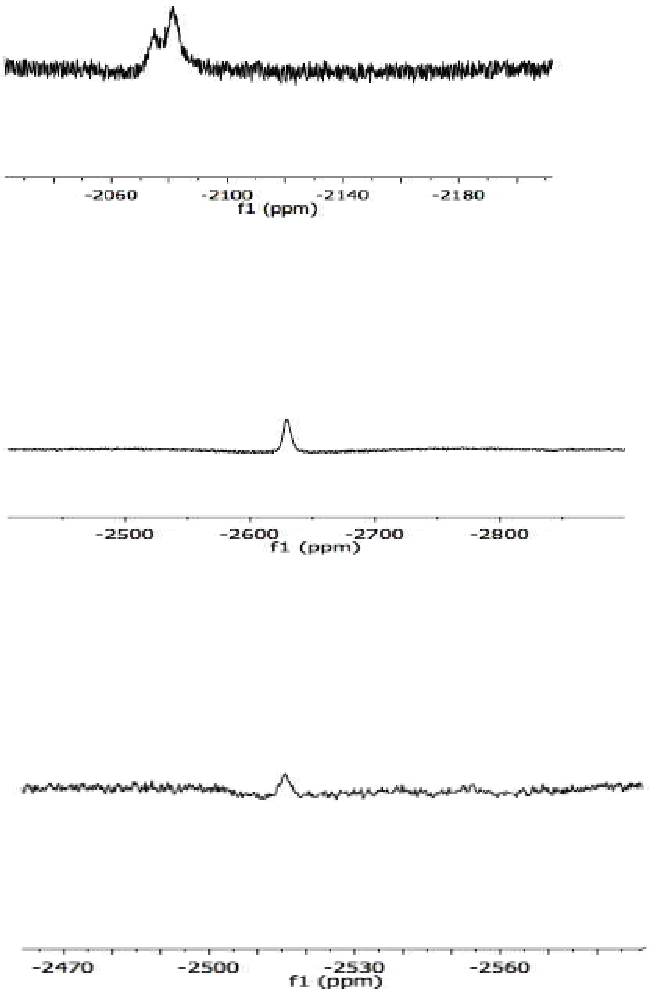

Figure 2.1. Top: ^{195}Pt NMR of [Pt(en)Cl(DMF)]NO_3 in THF-d^4/DMF. Middle: ^{195}Pt NMR of [Pt(en)Cl(piperonylamine)]NO_3 in D_2O. Bottom: ^{195}Pt NMR of [Pt(en)Cl(piperonyl)]NO_3 in D_2O + dGMP in D_2O.

2.2. Results and Discussion

2.2.1 Synthesis of 1 and its reaction with dGMP

Compound **1** was synthesized by the reaction of benzo[*d*][1,3]dioxol-5-ylmethanamine with [(en)$PtCl_2$] via halide abstraction in dimethylformamide (Scheme **2.1,** synthesis of compound **1**).

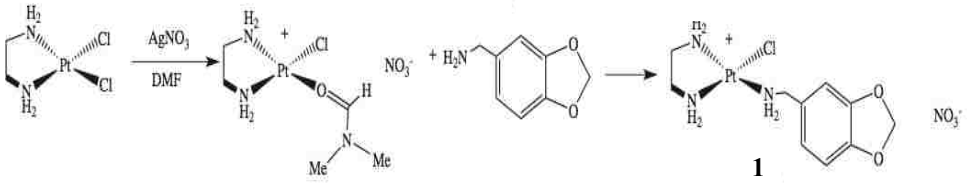

Scheme 2.1. Synthesis of compound [Pt(en)Cl(piperonylamine)]NO_3, by the reaction of [(en)$PtCl_2$] to $AgNO_3$ in DMF, followed by piperonylamine.

The compound was characterized by ^{1}H, ^{195}Pt-NMR and mass spectrometry. The ^{195}Pt NMR of the DMF intermediate complex showed two overlapping resonances in DMF/THF-d^8, which we attribute to a mixture of the DMF and THF- d^8 complexes (Figure **2.1**, top). To this solution was added 0.8 equivalents of piperonylamine, the solution evaporated to dryness and dissolved in D_2O. The ^{195}Pt-NMR showed a single peak at -2625 ppm relative to chloroplatinic acid (Figure **2.1**, middle).[22]

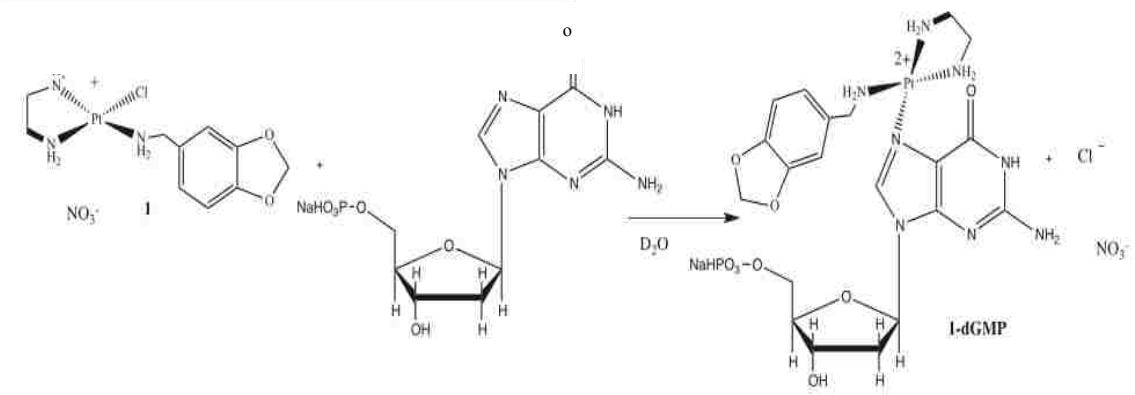

Scheme 2.2. The formation of adduct of compound **1** and dGMP in D_2O, where R=piperonylamine ($C_8H_7O_2$).

To this solution of compound **1** was added an equimolar (based on the piperonylamine) amount of dGMP and a shift to -2511 ppm was observed (Figure **2.1**, bottom). This gives evidence for the formation of a single adduct of compound **1** with dGMP**.**

2.2.2 The reaction of compound 1 with dGMP followed by ^{1}H-NMR

Equimolar solutions of compound **1** and dGMP were combined in D_2O and the reaction followed by ^{1}H-NMR over the course of 24 h using solvent suppression for the HDO peak (Figure **2.2**). Resonances assignable to residual DMF are observed at 8.3 ppm (CH), 2.3 and 2.4 ppm (2 Me). Thirty minutes after addition of the dGMP a new resonance appears at 8.5 ppm to low field of the H(8) of dGMP at 7.9 ppm appears which we assign to the formation of the adduct compound **1-dGMP** (Scheme **2.2.** formation of adduct of compound **1** and dGMP).

With increasing time the resonance at 7.9 ppm continues to decrease while the resonance at 8.5 ppm. After 19 h the resonance at 7.9 ppm has completely disappeared and only the peak assignable to compound **1-dGMP** is observed accompanied by the DMF resonance at 8.3 ppm in the downfield region of the spectrum. Other changes in the resonances above 7.0 ppm are also observed.

Figure 2.2

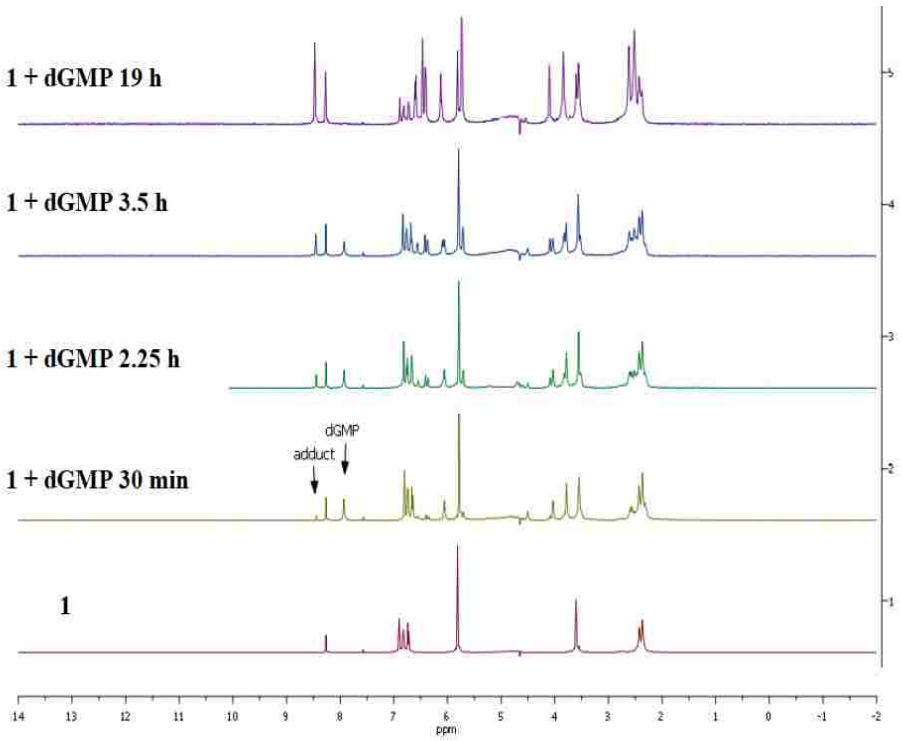

Figure 2.2. ^{1}H-NMR of compound **1** + equimolar dGMP versus time.

2.2.3 Transmission electron microscopy of compound 1 incubated with ssDNA GACT repeat

Based on these results compound **1** was incubated with a 25 mmol solution of a single-stranded GATC repeat (60 bases in length) at 40 ^{o}C for 6 hours in aqueous phosphate buffer using a six-fold molar excess of label (compound **1**) relative to the number of guanines. After dialysis to remove excess label, a micro drop of the solution was subjected to the stretching and straightening technique developed by Halcyon Molecular.[11]

Multiple strands were deposited on glass slide, sprayed with carbon and imaged on the 300 kV VG Microscope at Oak Ridge National Lab.[23]

Figure **2.3** shows a TEM image of a segment of the labeled GATC repeat. There are 15 G bases in the segment using the calculated value 0.77 nm/base and 11 of them are labeled (green dots). There are several labels that are out of sequence (red dots) and these could be labeled adenines.[21]

2.2.4 ^{1}H-NMR studies of compound 1 with dAMP

In order to test this hypothesis the reaction of dAMP with compound **1** was studied. The ^{1}H-NMR of equimolar amounts of dAMP and compound **1** in D_2O was followed over a 24 h period using water suppression. Although evidence of reaction is observed in the form of new resonances appearing in the downfield (8 ppm) and upfield (2-7 ppm) regions of the spectrum the H(8) of the adenine is still present after 24 h (Figure **2.4**). Thus the reaction **1** with dAMP is much slower than with dGMP and appears to be less specific, given the greater number new

resonances that appeared over the 24 h period. Nonetheless, this experiment does lend credence to the idea that the outlier labels (red dots) are compound **1-dAMP** although it is not clear if this product has the same structure as compound **1-dGMP** (Scheme **2.2**).

Figure 2.4

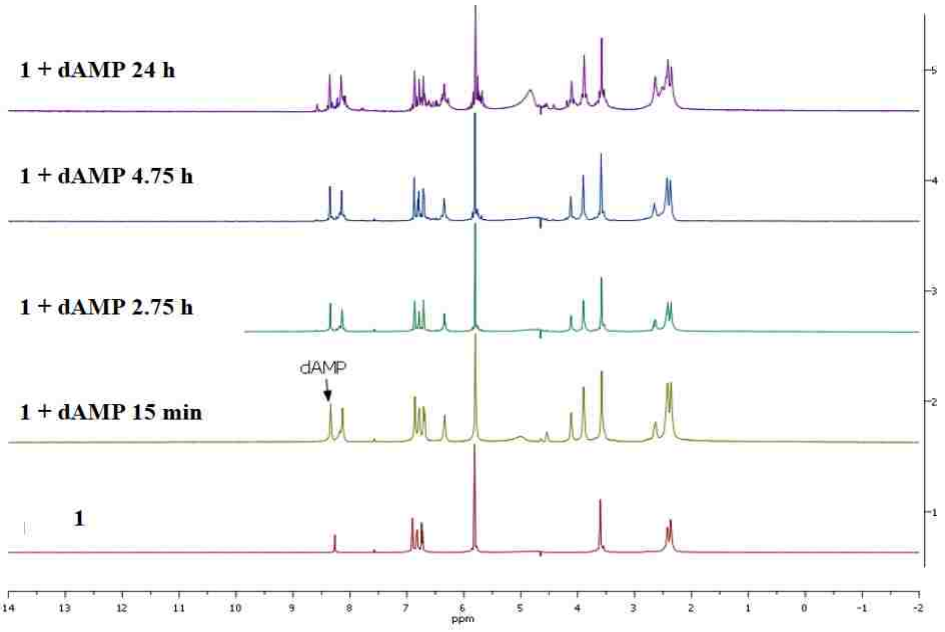

Figure 2.4. ^{1}H NMR studies of compound **1** + equimolar dAMP versus time.

2.2.5 Kinetic studies of amine variants compounds 2-7 with dGMP

The TEM experiment constitutes a proof of concept result in that it is possible to visualize a single platinum atom with base selectivity bound to stretched single-strand DNA. However, for

this labeling scheme to be effective the reaction of compound **1** with dGMP must be much faster. To this end a study of the rates of reaction of a series of complexes related to compound **1**, $Pt(en)Cl(NH_2R)]^+NO_3$ where R= $C_8H_{11}N$ (phenethylamine) (**2**), C_7H_9N (benzylamine (**3**), C_6H_7N (aniline) (**4**), C_6H_6IN (*p*-iodo-aniline) (**5**) C_3H_9NO (2-methoxy-ethylamine) (**6**) and $C_6H_{13}N$

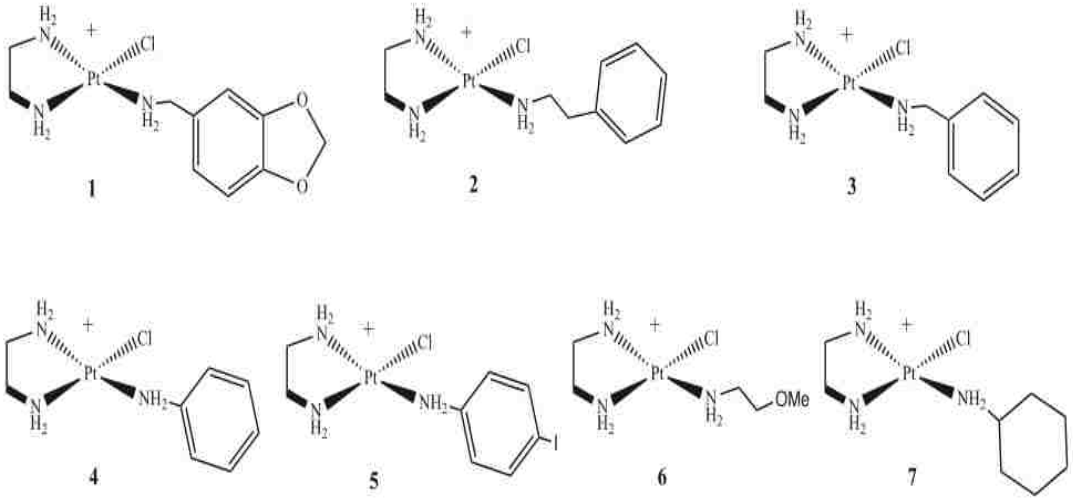

Figure Variants of Pt-amine complexes

(cyclohexylamine) (**7**) were synthesized and their rates of reaction with dGMP were followed by ^{1}H-NMR (Figure **2.5**). The amines were chosen for their differences in steric bulk and basicity of the donor atom. In the case of compound **5** a second heavy atom was included to increase electron scattering to improve visualization of the label.

Figure 1.5

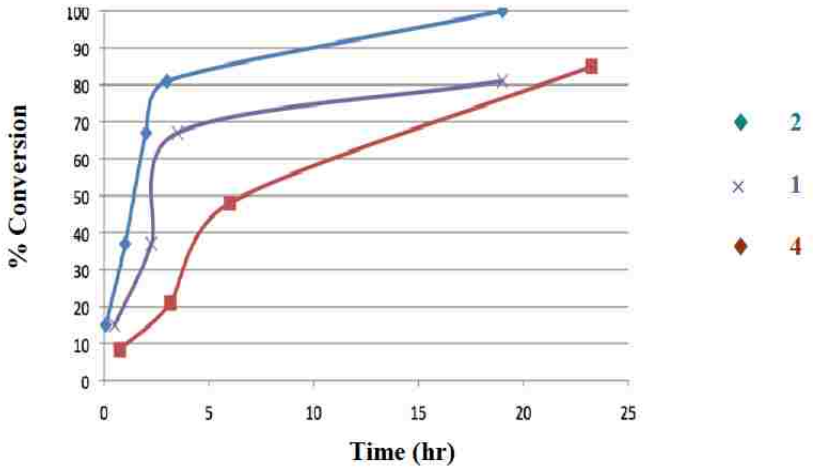

Figure 2.5. Kinetic plots of the reaction compound **1**, **2** and **4** with dGMP run at ambient temperatures in D_2O and based on integration of the adduct peak to the H(8) peak of dGMP.

Figure 2.3

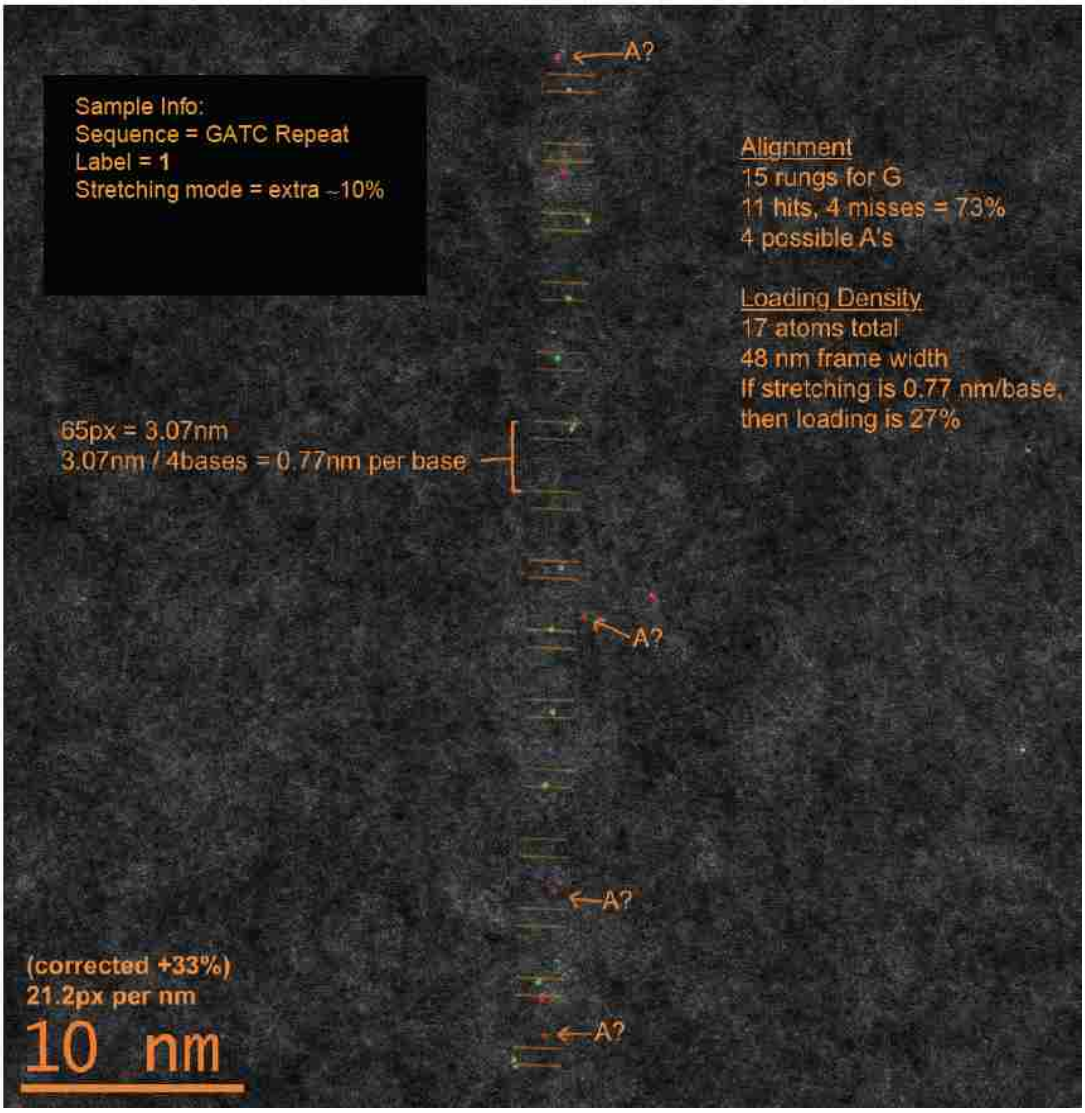

Figure 2.3. TEM multiple strand image of compound **1** incubated with a GACT repeat using a 300 kV VG Microscope at Oak Ridge National Lab.

The experiments were conducted with equimolar amounts of the amine complexes and dGMP in D_2O with water suppression. The reaction of compound **2** with dGMP is shown in Figure **2.5** and it can be seen that it reacts much more quickly than compound **1**, with the reaction being almost complete after just 2 h. Figure **2.6** compares the rate of conversion of compound **1** with **2** and **4**. Compound **3** showed the same rate of conversion as compound **1**, both being benzyl amines. Figure **2.7** compares the rate of conversion of **4** with **5** and shows that inclusion of the iodine atom does not have huge influence on the initial rate but does decrease the overall % conversion after 24 h. Complexes **6** and **7** reacted only sluggishly with dGMP and showed <50 % after 24 h.

Figure 2.6

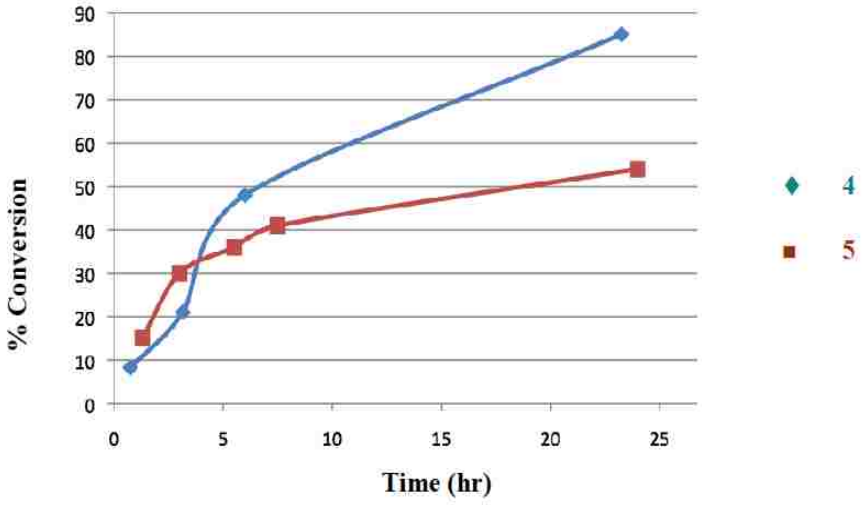

Figure 2.6. Kinetic plots of the reaction complexes **4** and **5** with dGMP run at ambient temperatures in D_2O and based on integration of the adduct peak to the H(8) peak of dGMP.

It is clear from these results that the longer tether in the phenethylamine complex results in the fastest rate of conversion and represents the best candidate for single metal atom labeling of guanine in single-stranded DNA.

The TEM results reported here for the labeling of GATC DNA with compound **1** using the stretching technique and the distance grid developed by Halcyon Molecular represents a proof of concept for visualizing a single platinum atom selectively bound to guanine.[11, 21]

The selectivity for guanine is based on the clear results of our studies in solution on the binding of compound **1** with dGMP. This selectivity is also based on our previous studies with dGMP and triosmium cluster labels.[16]

Outlier spots were observed in the TEM and were attributed to side reactions with adenine that could be due to either covalent bonding as with guanine or to non-specific electrostatic interactions. Following the reaction of dAMP with compound **1** resulted in much more complex changes in the ^{1}H-NMR of the dAMP relative to dGMP suggesting that there are several ways that the dAMP is interacting with the label (Figures **2.3** and **2.4**).

Although compound **1** was reasonably selective for guanine its reaction with dGMP was rather slow. Following the rates of the reactions of complexes **2**-**7** revealed some of the factors that control the rate of reaction of these Pt complexes with DNA. Compound **2**, the phenethylamine analogue showed fastest reactivity as observed by NMR spectroscopy. It was consumed in 2 h in comparison to compound **1**, which took 12 h at RT. Compound **3** reacted at the same rate as compound **1** being a benzylamine, illustrating that the dioxo ring has little influence on the rate of reaction with dGMP, but is preferred for its better water solubility. Compound **4** reacted more slowly than compounds **1** or **2** and taken together the results shown in Figure **2.5** suggest that tether length to the aromatic ring is the dominant factor in affecting the rate of reaction with

dGMP. The differences in basicity may also play a role but based on the results for the remaining compounds this is apparently of secondary importance. Compound **5** reacts more slowly than compound **4** and this may be due to the electron withdrawing effect of the iodo group (Figure **2.6**). This is unfortunate in that the iodo group would offer enhanced imaging possibilities. Compound **6** and **7** reacted very slowly and reaction with dGMP was <50% converted after 24 h. We tentatively assign this to steric considerations where the greater motional degrees of freedom of compound **6** and the relative bulkiness of the cyclohexyl group in compound **7** compared to phenyl interfere with the displacement of chloride by the dGMP.

2.3. Experimental

2.3.1 Materials and Methods

All amines, $Pt(en)Cl_2$ and dGMP were purchased from Sigma-Aldrich Chemicals and used as received. Deuterated solvents were purchased from Cambridge Isotopes Inc and used as received. DMF was distilled from calcium hydride directly before use. Other solvents were reagent grade and were purchased from J. T. Baker and used as received.

^{1}H, ^{195}Pt and ^{13}P NMR spectra were obtained on a Varian NMR system 500 MHz spectrometer at 500, 109.1 and 202.6 MHz respectively. Infrared spectra were obtained on a Thermo-Nicolet 633 FT-IR spectrometer. Prior to the NMR experiments all Pt complexes were purified on a Biotage (Isolera prime Flash purification system) using Chromobond Flash FM 15/2 C_{18}, 9 cm and Chromobond Flash FM 25/5 C18, 10 cm columns.

2.3.2 Synthesis of [(Pt(en)Cl(DMF)]NO_3

[Pt(en)Cl_2] (50 mg, 0.153 mmol) was suspended in DMF (5 mL) and $AgNO_3$ (24.8 mg, 0.146 mmol, 0.95 equiv.) in DMF (1 mL) was added. The solution was stirred for 16 h at room temperature in the dark and filtered through membrane filters (0.2μm) to remove AgCl.

2.3.3 Synthesis of [Pt(II)(piperonylamine)(en)Cl]$^+NO_3^-$ (1)

Piperonylamine (18.5 mg, 0.122 mmol, 0.8 equiv relative to [Pt(en)Cl_2]) was dissolved in xylene (12 mL) and added to the [Pt(en)Cl(dmf)]$^+$ NO_3^- solution. The mixture was stirred overnight at 40 ^oC. Solvents were removed *in vacuo* and the remaining product was redissolved in a minimum amount of Milli-Q water and stored overnight at 4 ^oC. Insoluble yellow particles of residual [Pt(en)Cl(dmf)]$^+$ NO_3^- were removed by filtration through membrane filters (0.2 μm). The clear filtrate was lyophilized to give the final product, compound (**1**), in approximately 45%. ^{1}H NMR (D_2O, 500 MHz, 298 K): δ 2.2 (s, 3NH_2, en), 2.6 (s, en), 3.6 (s, CH_2), 5.8 (s, CH_2 ppr), 6.7 (s, CH, Ar), 6.8 (s, CH,Ar), 6.9 (s, CH,Ar). ^{195}Pt NMR (D_2O, 500 MHz, 298 K) δ -2624.8. MS (ES): m/z 443.

2.3.4 Reaction of [Pt(II)(piperonylamine)(en)Cl]$^+NO_3^-$ (1) with 1-dGMP

In an NMR tube compound **1** (4.5 mg, 0.089 mmol, 1 equiv.) and dGMP (3.0 mg, 0.089 mmol, 1 equiv.) were mixed in 0.5 ml D_2O. The mixture was kept overnight at 40 ^oC. ^{195}Pt-NMR a new peak at -2511 ppm observed and -2625 ppm peak disappeared completely. In a separate reaction

when the reaction was followed by ^{1}H NMR a new peak appeared at δ 8.2 and 7.9 H(8) peak disappeared completely.

2.3.5 Synthesis of [Pt(II)phenethylamine(en)Cl](NO$_3$) (2)

Phenethylamine (14.7 mg, 0.122 mmol, 0.8 equiv.) was dissolved in xylene (12 mL) and added to the [Pt(en)Cl(NO$_3$)] (0.122 mmol) solution. ^{1}H-NMR (D_2O, 500 MHz, 298 K): δ 2.2 (s, $3NH_2$), 2.4 (s, en), 2.8 (s, CH_2), 2.9 (s, CH_2), 7.2 (m, CH_{phy}), 7.4 (m, CH_{phy}). MS (ES): m/z 412.

2.3.6 Synthesis of [Pt(II)benzylamine(en)Cl](NO$_3$) (3)

Benzylamine (13.07 mg, 0.122 mmol, 0.8 equiv.) was dissolved in xylene (12 mL) and added to the [Pt(en)Cl(DMF)]NO_3 (0.122 mmol) solution . ^{1}H-NMR (D_2O, 500 MHz, 298 K): δ 2.0 (s, $3NH_2$), 2.8 (t, en), 3.8 (s, CH_2), 7.3 (m, CH, Ar). MS (ES): m/z 399.

2.3.7 Synthesis of [Pt(II)aniline(en)Cl](NO$_3$) (4)

Aniline (11.36 mg, 0.122 mmol, 0.8 equiv.) was dissolved in xylene was dissolved in xylene (12 mL) and added to the [Pt(en)Cl(DMF)]NO_3 (0.122 mmol) solution. ^{1}H NMR (D_2O, 500 MHz, 298 K): δ 2.0 (s, $3NH_2$), 2.8 (t, en), 6.6 (m, CH, Ar), 6.8 (m, CH, Ar), 7.2 (m, CH, Ar). MS (ES): m/z 385.

2.3.8 Synthesis of [Pt(II)(4-iodoaniline)(en)Cl](NO$_3$) (5)

4-iodoaniline (27.72 mg, 0.122 mmol, 0.8 equiv.) was dissolved in xylene (12 mL) and added to the [Pt(en)Cl(NO_3)] (0.122 mmol) solution. ^{1}H-NMR (D_2O, 500 MHz, 298 K): δ 2.0 (s, $3NH_2$), 2.8 (t, en), 6.4 (m, CH, Ar), 7.4 (m, CH, Ar). MS (ES): m/z 511.

2.3.9 Synthesis of [Pt(II)(2-methoxyethanamine)(en)Cl](NO_3) (6)

2-methoxyethanamine (9.16 mg, 0.122 mmol, 0.8 equiv.) was dissolved in xylene (12 mL) and added to the [Pt(en)Cl(NO_3)] (0.122 mmol) solution. ^{1}H-NMR (D_2O, 500 MHz, 298 K): δ 2.0 (s, $3NH_2$), 2.7 (t, CH_2), 2.8 (s, en), 3.3 (s, CH_3), 3.8 (t, CH_2). MS (ES): m/z 377.

2.3.10 Synthesis of Pt(II)(cyclohexylamine)(en)Cl(NO_3) (7)

Cyclohexylamine (12.34 mg, 0.122 mmol, 0.8 equiv.) was dissolved in xylene (12 mL) and added to the [Pt(en)Cl(DMF)]NO_3 (0.122 mmol) solution. ^{1}H-NMR (D_2O, 500 MHz, 298 K): δ 1.1 (m, CH_{2Hex}), 1.5 (m, CH_{2Hex}), 1.7 (m, CH_{2Hex}), 2.0 (s, $3NH_2$), 2.7 (m, CH), 2.8 (s, en), 3.3 (s, CH_3), 3.8 (t, CH_2). MS (ES): m/z 391.

2.4. Conclusions

The relative rates reported here for the reactions of compounds **1**-**7** with dGMP could prove useful for future applications of the reactions of Pt complexes with DNA. The visualization of compound **1** attached to a stretched single stranded DNA is proof of concept for the application

of high-powered TEM for visualization of single metal atoms attached to bio-macromolecules.

Chapter 3: Synthesis and dGMP binding of a Pt-triosmium conjugate label for sequencing by TEM Imaging

3.1. Introduction

The interaction of benzoheterocycle complexes of triosmium carbonyl clusters were investigated in our lab. [14-16] These studies revealed some of the structural requirements for selective binding of modified triosmium clusters with guanosine monophosphate (dGMP). Selectivity for guanine over the other bases was also observed. [14, 15] However, subsequent attempts to obtain a straight and stretched single stranded DNA containing a covalently bound triosmium cluster failed.[16]

In the previous chapter on the synthesis of guanine selective compound for DNA sequencing using electron microscopy, we developed a guanine base selective platinum compound, $[Pt(en)Cl(NH_2R)]^+NO_3^-$, where R= $C_8H_9NO_2$ (benzo[*d*][1,3]dioxol-5-ylmethanamine) compound **1**. Compound **1**, which is a big step in right direction for guanine selective labeling of DNA, requires the use of high resolution TEM (HRTEM; resolution ≤ 0.5 Å) for sequencing. It may be noted again that heavy metal (Z > 70) staining is well-known to increase image contrast in EM. The relative number of electrons that are scattered to a detector is approximately proportional to $Z^{1.5}$. This suggests that a trimetallic or terametallic cluster would provide a more useful signal than a single heavy metal atom. The present study focuses on studying the synthesis and binding of clusters to base-selectively label DNA via covalent bonding for high throughput genetic sequencing using electron microscopy. This research discusses the synthesis of tetrametallic compounds, by attaching triosmium cluster compounds to the guanine-selective platinum

compound, with the precursor of compound **1** $[Pt(en)Cl(DMF)]NO_3$, as reported in chapter 2. The conjugate triosmium-Pt compound, now tetrametallic, would serve as a potential label for DNA sequencing by low resolution TEM, further bringing down the sequencing cost significantly. It is proposed to synthesize the compound $[Os_3(CO)_{10}PPh_2(CH_2)_2NH_2(en)PtCl]NO_3$, compound **9** that contains Pt as a linker to label guanine. The synthesis was performed by reacting $Os_3(CO)_{10}(CH_3CN)_2$ with $Ph_2PCH_2CH_2NH_2$ which yielded η^2 chelate complex $Os_3(CO)_{10}PPh_2(CH_2)_2NH_2$, compound **8**. Compound **8** was reacted with $[(en)PtCl(DMF)]NO_3$ in a CO atmosphere to give compound **9**. A solution of **9** was then combined with an equimolar amount of dGMP, ^{1}H- and ^{195}Pt-NMR gave evidence of formation of an adduct with dGMP. The solid-state structure of compound **8** is also reported.

3.2. Results and Discussion

The Pt and Os based complexes were synthesized in our lab, which provided enough evidence that it reacts selectively on N-7 of guanine. The compound $[Os_3(CO)_{10}PPh_2(CH_2)_2NH_2(en)PtCl]NO_3$, compound **9** was synthesized by reacting activated $Os_3(CO)_{11}(CH_3CN)$ with 2-diphenylphosphine-ethylamine to yield a cyclized amino-phosphine complex that undergoes ring opening on reaction with carbon monoxide and then complexes with [Pt(en)Cl-DMF](Scheme **3.1**) (Figure **3.1**). Preliminary ^{1}H-NMR studies reveal similar behavior to the triosmium alkyne mesylate complex where disappearance of the H(8) resonance is observed along with the appearance of new resonances in the upfield region.[16]

The appeal of this approach is that the amino phosphine can be complexed to almost any polynuclear carbonyl complex (e.g. $Ir_4(CO)_{12}$) making it a more general approach than the use of the functionalized alkyne mesylates.

However, the limited solubility caused a significant problem in ^{1}H-NMR spectroscopy. To avoid this problem, in house synthesized water-soluble ligands $[C_{18}H_{12}O_9PS_3]Na_3$ (trinegative) and $[C_{15}H_{39}N_3O_3P]I_3$ (triposivite) were incorporated onto the complex. Which made the complex highly water-soluble. However, compounds carrying charged groups showed electrostatic interaction with negatively charged phosphate backbone. The positively charged compound caused cross-linking of oligos, which was observed under the microscope and also no clear changes were observed of the reaction with mononucleaotide in ^{1}H-NMR. As soon as the label solution was added to the ssDNA-oligo solution, strands started to form a globular structure. Whereas, negatively charged compound showed significantly slow reactivity towards mononucleotide, may be due to repulsive interaction between the negatively charged compound and the phosphate group.

The insolubility of mononucleotide in any organic solvents and insolubility of these compounds in water made tough to pursue with cluster complex at the moment.

3.2.1 Synthesis and structure $[Os_3(CO)_{10}PPh_2(CH_2)_2NH_2]$ compound 8

In the hope of combining the effectiveness of the two- carbon tether with a metal cluster label we synthesized the compound $[Os_3(CO)_{10}PPh_2(CH_2)_2NH_2(en)PtCl]NO_3$ using the bidentate ligand 2-diphenylphosphino-ethylamine (Scheme **3.1**). Activated osmium cluster $Os_3(CO)_{11}(CH_3CN)$ was reacted with 2-diphenylphosphino-ethylamine at ambient temperature in methylene chloride. The spectroscopic data indicated that the reaction had resulted in the displacement of a carbonyl ligand to give $[Os_3(CO)_{10}PPh_2(CH_2)_2NH_2]$ compound **8** (Scheme **3.1**). However, we could not determine if the ligand was coordinated in a bridging or chelating mode and so a solid-state

structure was undertaken. The solid-state structure of compound **8** is shown in Figure **3.1** with selected bond lengths and angles in the figure caption. The crystal and collection data are given in Table **3.1**. The 2-diphenylphosphino-ethylamine ligand is chelated to one Os atom. There is considerable precedent in the literature for the chelate structure being preferred for bidentate ligands with an ethylene bridge in the chemistry of triosmium clusters. However, the equilibrium between the chelate and two metal atom bridging structure is highly dependent on the nature of the of the two donor atoms, i. e. (PP), (PS), (PN) or (PO).[24-27]

The structure of compound **8** consists of an Os triangle with the chelating diphenylphosphino-2-ehtyl amine ligand on Os(3). The Os(2)-Os(3) bond length is slightly shorter than (2.86(2) Å) than the other two Os-Os bonds (2.91(2) Å). The Os(3)-P(1) and Os(3)-(N1) bond lengths (2.32(2) and 2.25(2) Å, respectively are fairly typical of these bonds in triosmium clusters. [25-28]

3.2.2 Conversion of compound 8 to $[Os_3(CO)_{11}PPh_2(CH_2)_2NH_2(en)PtCl]NO_3$ compound 9 and attempted reaction with dGMP

The opening of the chelate ring at the Os(3)-N(1) bond could be accomplished by treating compound **8** with CO gas at 50 ^oC in THF-d^8. The reaction is followed by ^{31}P-NMR and after one hour the ^{31}P-NMR resonance at 33.70 ppm, assigned to compound **8,** is replaced by a new resonance at 35.55 ppm. To the THF solution was added an equimolar amount of $[Pt(en)Cl(DMF]NO_3$. The Pt-cluster adduct was isolated by preparative reverse phase TLC and characterized by IR and NMR spectroscopies as $[Os_3(CO)_{11}PPh_2(CH_2)_2NH_2(en)PtCl]NO_3$ compound **9**.

A solution of compound **9** was then combined with an equimolar amount of dGMP in 90:10 (v/v) D_2O:MeOH. After 4 h there was some evidence of formation of an adduct as noted by the appearance of a new resonance at 8.6 ppm downfield of the H(8) resonance of guanine as noted for the other dGMP adducts reported here. However with increasing time a precipitation was noted and the overall intensity of the NMR resonances increased. Thus it appears that if **dGMP-compound 9** in this solvent mixture was too limited to make further studies possible.

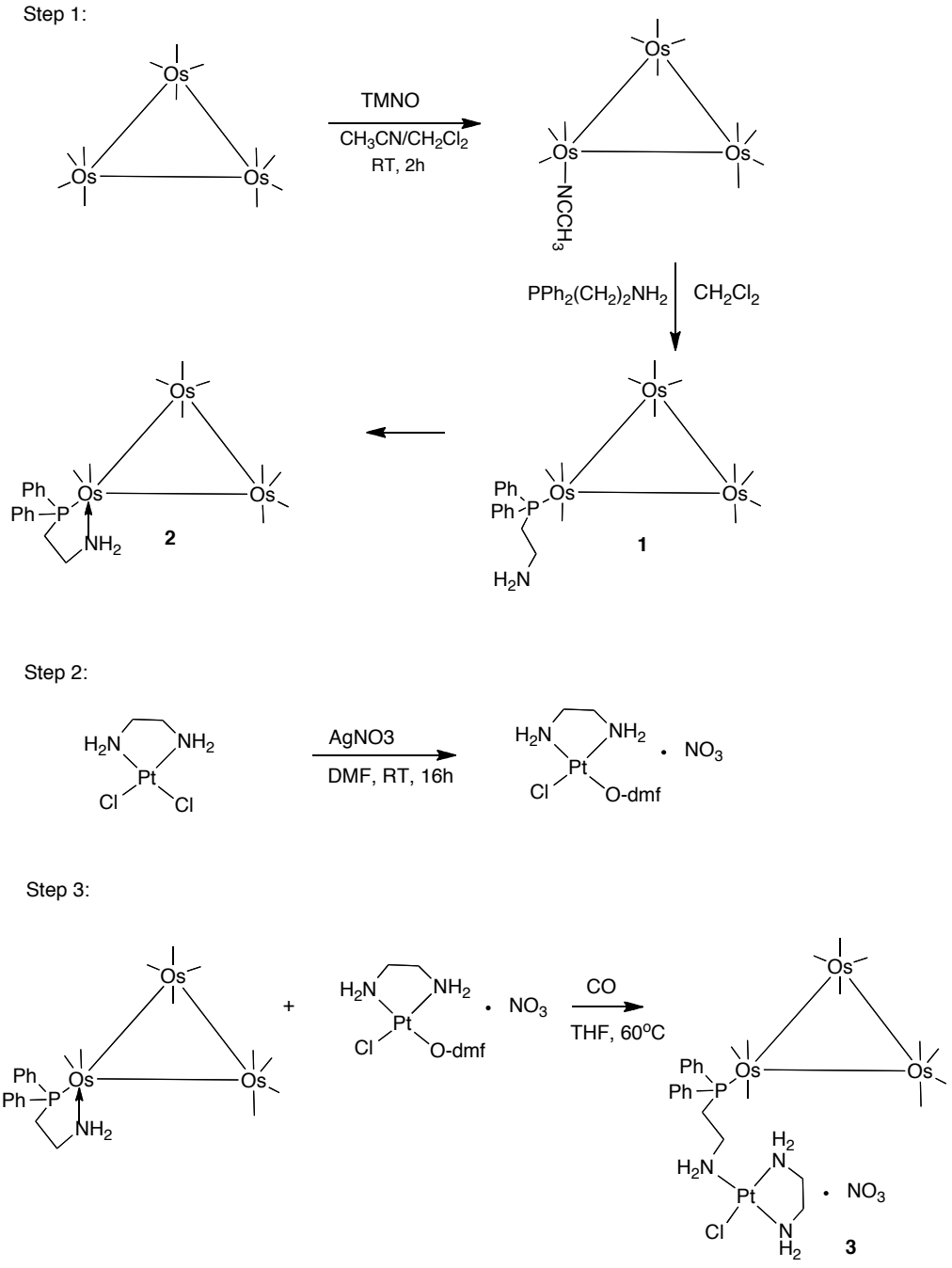

Scheme 3.1. Stepwise synthesis of $[Os_3(CO)_{10}PPh_2(CH_2)_2NH_2(en)PtCl]NO_3$, a guanine selective label.

3.3. Experimental

3.3.1 Materials and Methods

TMAO (trimethylamine N-oxide), $Pt(en)Cl_2$ and dGMP, dTMP, dCMP and dAMP were purchased from Sigma-Aldrich Chemicals. Triosmimum dodecacarbonyl ($Os_3(CO)_{12}$) and diphenylphosphino-2-ethylamine ($PPh_2(CH_2)_2NH_2$) were purchased from Strem Chemicals. Solvents and other reagents were of reagent grade and were purchased from J. T. Baker and used as received. Acetonitrile was distilled from calcium hydride directly just before use. Syntheses of the Os-cluster compounds carried out under a nitrogen atmosphere, but purification processes were carried out in air using preparative thin layer chromatography (20×20 cm plates coated with 500 μm silica or C-18 reverse phaseon silica ordered from Dynamic Absorbents Inc).

^1H- and ^{13}P-NMR spectra were obtained on a Varian NMR system 500 MHz spectrometer at 500 and 202.6 MHz respectively. Infrared spectra were obtained on a Thermo-Nicolet 633 FT-IR spectrometer.

3.3.2 Synthesis of $[Os_3(CO)_{10}PPh_2(CH_2)_2NH_2$, compound 8

$[Os_3(CO)_{11}(NCCH_3)]$ (370 mg, 0.402 mmol) was dissolved in 10 mL CH_2Cl_2 and $PPh_2(CH_2)_2NH_2$ (0.092 mg, 0.402 mmol) was added. The solution was stirred at room temperature for overnight. Analytical thin layer chromatography (30% CH_2Cl_2 and 70% hexane (v/v) as eluent) was used to confirm complete conversion. The solution was rotary evaporated under vacuum to dryness. Two bands were observed on preparative TLC. Faster moving band R_f = 0.6 was identified by solid-state structure, ^{31}P- and ^1H-NMR, as a cyclized amino-phosphine $Os_3(CO)_{10}PPh_2(CH_2)_2NH_2$, compound **8**. The slow moving band R_f = 0.1 could not be analyzed

due to unresolved NMR spectroscopy. Yield for compound **8**: 45%. IR (ν(CO) in KBr: 2079 m, 2028 s, 2004 m, 1974 w cm^{-1}. ^{1}H-NMR (500MHz in CH_2Cl_2 at 25^{o}C) 7.53 (m, 3H, H(3,4,5)) , 7.42 (m, 2H, H(2,6)), 2.43 (s (NH_2)), 1.56 (m, 2H, $CH_2\beta$-NH_2), 1.09 (m, 2H, $CH_2\alpha$-NH_2). ^{13}C-NMR (CH_2Cl_2): 187.35 (s, 4CO, 2Os), 187.45 (s, 4CO, 2Os), 183.95 (s, 2CO, 1Os). ^{31}P-NMR (CH_2Cl_2): 33.70 (s, 1P, $PPh_2(CH_2)_2NH_2$).

3.3.3 Solid-state structure determination of 8

A yellow plate 0.07 x 0.05 x 0.04 mm in size was mounted on a Cryoloop with Paratone oil. Data were collected in a nitrogen gas stream at 100(2) K using phi and omega scans. Crystal-to-detector distance was 60 mm and exposure time was 20 seconds per frame using a scan width of 1.0°. Data collection was 100.0% complete to 25.00° in θ. A total of 50804 reflections were collected covering the indices, -10<=*h*<=10, -17<=*k*<=17, -24<=*l*<=25. 4970 reflections were found to be symmetry independent, with an R_{int} of 0.0318. Indexing and unit cell refinement indicated a primitive, monoclinic lattice. The space group was found to be P2(1)/n (No. 14). The data were integrated using the Bruker SAINT software program and scaled using the SADABS software program. Solution by direct methods (SIR-97) produced a complete heavy-atom phasing model consistent with the proposed structure. All non-hydrogen atoms were refined anisotropically by full-matrix least-squares (SHELXL-97). All hydrogen atoms were placed using a riding model. Their positions were constrained relative to their parent atom using the appropriate HFIX command in SHELXL-97.

3.3.4 Chelate ring opening of compound 8 with CO complexation with [Pt(en)Cl(DMF)]NO_3 compound 9

40 mg (0.036 mmol) of compound **8** dissolved in THF-d^8 (10 mL) and CO gas was bubbled through the solution at 50°C for 1h. The reaction was monitored by ^{31}P-NMR spectroscopy the resonance at 33.70 ppm assignable to compound **8** shifted to 35.45 ppm, which we assign to the ring-opened compound, $[Os_3(CO)_{10}PPh_2(CH_2)_2NH_2]$. A solution of $[(en)PtCl(DMF)]NO_3$ (0.03 mmol) in 1.5 mL DMF was then added to the reaction flask and was stirred overnight at room temperature. The Pt-cluster adduct was then precipitated with diethyl ether to remove DMF and purified by reverse phase preparative TLC (50% MeOH, 50% CH_2Cl_2, v/v). One faint band was observed and isolated by extraction with methanol and rotary evaporation. 35 mg (0.023 mmol) of a greenish-brown solid was obtained (Yield = 33%), whose spectroscopic data is consistent with $[Os_3(CO)_{10}PPh_2(CH_2)_2NH_2(en)PtCl]NO_3$, compound **9**. (ν(CO) in KBr: 1966 m, 2003 s, 2047 m, 2081 w cm^{-1}. ^{1}H-NMR (500 MHz in CD_3OD at 25°C) 7.8-8.2 (broad m, 12H, Phen), 5.9 (s, 2H, NH_2), 3.6 (s, 2H, CH_2-P), 3.1(t, 4H, en), 1.6 (s, 2H, CH_2-N). ^{31}P-NMR (CD_3OD) 35.55.

3.3.5 Reaction between dGMP and $[Os_3(CO)_{10}PPh_2(CH_2)_2NH_2(en)PtCl]NO_3$ compound 9

Equimolar molar amounts of dGMP (0.023 mmol) and $[Os_3(CO)_{10}PPh_2(CH_2)_2NH_2(en)PtCl]NO_3$ (0.023 mmol) were added in CD_3OD and D_2O (90:10, v/v). Reaction was followed by ^{1}H-NMR. Some conversion to **dGMP-compound 9** was observed after 4 h as noted by the decrease in H(8) resonance of dGMP and the appearance of a new resonance at 8.6 ppm. However, due to precipitation of either the **dGMP-compound 9** or compound **9**, the kinetics of conversion rate could not be followed precisely.

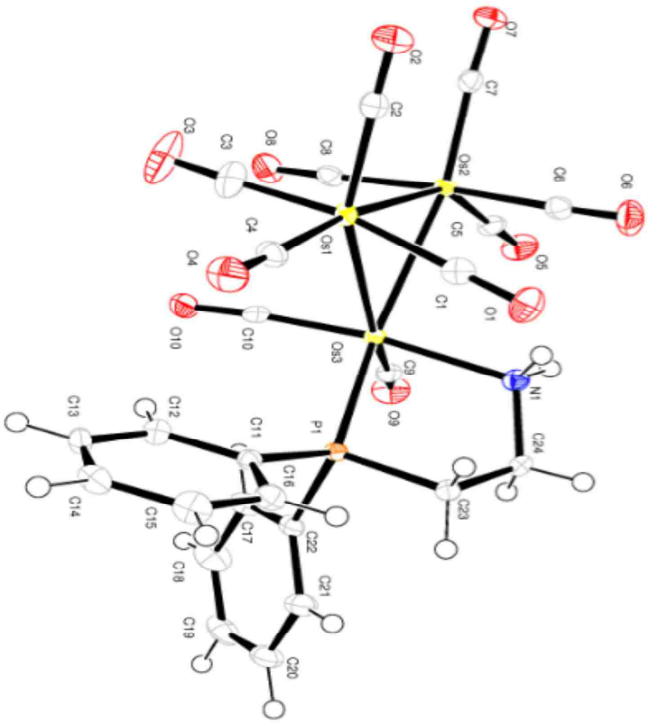

Figure 3.1. Solid-state structure of $[Os_3(CO)_{10}PPh_2(CH_2)_2NH_2]$ (8). Selected bond distances: N(1)-Os(3), 2.249(3); N(1)-H(1A), 0.9200; N(1)-H(1B), 0.9200; P(1)-Os(3), 2.3206(9); Os(1)-Os(2), 2.9028(2); Os(1)-Os(3), 2.9151(2); Os(2)-Os(3), 2.8626(2) Å. Average CO bond distance: 1.147(5) Å. Average Os-C-O bond angle: 176.1(3) deg.

3.4. Conclusions

The synthesis of complexes **8** and **9** $[Pt(en)Cl(NH_2R)]^+NO_3^-$ opens the way for the labeling of DNA bases with clusters attached to a platinum complex. Preliminary ^1H NMR studies reveal similar behavior to the triosmium alkyne mesylate.[16] complex where disappearance of the H(8) resonance was observed. The appeal of this approach is that amino phosphine can be complexed to almost any polynuclear carbonyl complex (e.g. $Ir_4(CO)_{12}$) making it a more general approach than the use of the functionalized alkyne mesylate. The approach outlined here represents just a few of many ways to conjugate polymetallic cluster to functional groups capable of selective binding to nucleotides.

Appendices

Table **3.1.** Crystal data and structure refinement for compound **8**.

Empirical formula	C24 H16 N O10 Os3 P	
Formula weight	1079.95	
Temperature	100(2) K	
Wavelength	0.71073 Å	
Crystal system	Monoclinic	
Space group	P2(1)/n	
Unit cell dimensions	a = 8.9448(3) Å	α= 90°.
	b = 14.7147(4) Å	β= 101.5820(10)°.
	c = 20.9890(7) Å	γ = 90°.
Volume	2706.32(15) $Å^3$	
Z	4	
Density (calculated)	2.651 Mg/m^3	
Absorption coefficient	14.165 mm^{-1}	
F(000)	1960	
Crystal size	0.07 x 0.05 x 0.04 mm^3	
Crystal color/habit	yellow plate	
Theta range for data collection	1.70 to 25.39°.	
Index ranges	-10<=h<=10, -17<=k<=17, -24<=l<=25	
Reflections collected	50804	
Independent reflections	4970 [R(int) = 0.0318]	
Completeness to theta = 25.00°	100.0 %	
Absorption correction	Semi-empirical from equivalents	
Max. and min. transmission	0.6011 and 0.4372	
Refinement method	Full-matrix least-squares on F^2	
Data / restraints / parameters	4970 / 0 / 352	
Goodness-of-fit on F^2	1.128	
Final R indices [I>2sigma(I)]	R1 = 0.0150, wR2 = 0.0299	
R indices (all data)	R1 = 0.0187, wR2 = 0.0315	

Largest diff. peak and hole	0.844 and -0.798 e.Å^{-3}

Table **3.2.** Atomic coordinates (x 10^4) and equivalent isotropic displacement parameters ($Å^2$x 10^3) for compound **8**. U(eq) is defined as one third of the trace of the orthogonalized U^{ij} tensor.

	x	y	z	U(eq)
C(1)	2485(4)	2656(3)	1603(2)	18(1)
C(2)	284(4)	1905(3)	498(2)	20(1)
C(3)	833(4)	271(3)	1161(2)	27(1)
C(4)	87(4)	1720(3)	1862(2)	20(1)
C(5)	6168(4)	913(3)	751(2)	18(1)
C(6)	4490(4)	2473(3)	737(2)	18(1)
C(7)	3223(4)	1284(3)	-230(2)	18(1)
C(8)	3565(4)	-110(3)	708(2)	18(1)
C(9)	6384(4)	404(3)	2234(2)	18(1)
C(10)	3539(4)	-129(3)	2070(2)	18(1)
C(11)	2477(4)	1325(2)	3390(2)	13(1)
C(12)	1634(4)	520(3)	3331(2)	20(1)
C(13)	298(4)	466(3)	3563(2)	21(1)
C(14)	-229(4)	1212(3)	3853(2)	21(1)
C(15)	586(5)	2015(3)	3906(2)	24(1)
C(16)	1942(4)	2076(3)	3676(2)	19(1)
C(17)	5790(5)	-283(3)	3641(2)	22(1)
C(18)	6607(5)	-826(3)	4134(2)	29(1)
C(19)	7103(5)	-474(3)	4748(2)	29(1)
C(20)	6763(5)	416(3)	4881(2)	28(1)
C(21)	5931(4)	957(3)	4398(2)	21(1)
C(22)	5452(4)	614(3)	3767(2)	15(1)
C(23)	5052(4)	2472(2)	3254(2)	16(1)
C(24)	6357(4)	2561(3)	2890(2)	17(1)
N(1)	5776(3)	2314(2)	2193(1)	15(1)
O(1)	2985(3)	3359(2)	1776(1)	26(1)
O(2)	-445(4)	2146(2)	17(2)	35(1)
O(3)	346(4)	-445(2)	1066(2)	49(1)
O(4)	-829(3)	1875(2)	2155(1)	30(1)

O(5)	7442(3)	772(2)	794(1)	28(1)
O(6)	4780(4)	3221(2)	743(1)	30(1)
O(7)	2817(3)	1356(2)	-783(1)	27(1)
O(8)	3323(4)	-870(2)	707(1)	28(1)
O(9)	7481(3)	-33(2)	2313(1)	27(1)
O(10)	3050(3)	-850(2)	2110(1)	26(1)
P(1)	4303(1)	1316(1)	3129(1)	11(1)
Os(1)	1514(1)	1533(1)	1312(1)	13(1)
Os(2)	4062(1)	1176(1)	682(1)	12(1)
Os(3)	4483(1)	993(1)	2065(1)	11(1)

Table **3.3.** Bond lengths [Å] and angles [°] for compound **8**.

C(1)-O(1)	1.156(5)	C(15)-C(16)	1.395(5)
C(1)-Os(1)	1.909(4)	C(15)-H(15)	0.9500
C(2)-O(2)	1.141(5)	C(16)-H(16)	0.9500
C(2)-Os(1)	1.917(4)	C(17)-C(22)	1.391(5)
C(3)-O(3)	1.142(5)	C(17)-C(18)	1.393(5)
C(3)-Os(1)	1.961(4)	C(17)-H(17)	0.9500
C(4)-O(4)	1.142(5)	C(18)-C(19)	1.377(6)
C(4)-Os(1)	1.906(4)	C(18)-H(18)	0.9500
C(5)-O(5)	1.144(5)	C(19)-C(20)	1.385(6)
C(5)-Os(2)	1.900(4)	C(19)-H(19)	0.9500
C(6)-O(6)	1.131(5)	C(20)-C(21)	1.383(6)
C(6)-Os(2)	1.946(4)	C(20)-H(20)	0.9500
C(7)-O(7)	1.150(4)	C(21)-C(22)	1.400(5)
C(7)-Os(2)	1.917(4)	C(21)-H(21)	0.9500
C(8)-O(8)	1.139(5)	C(22)-P(1)	1.835(4)
C(8)-Os(2)	1.947(4)	C(23)-C(24)	1.523(5)
C(9)-O(9)	1.156(5)	C(23)-P(1)	1.828(4)
C(9)-Os(3)	1.878(4)	C(23)-H(23A)	0.9900
C(10)-O(10)	1.157(5)	C(23)-H(23B)	0.9900
C(10)-Os(3)	1.856(4)	C(24)-N(1)	1.495(5)
C(11)-C(16)	1.388(5)	C(24)-H(24A)	0.9900
C(11)-C(12)	1.396(5)	C(24)-H(24B)	0.9900
C(11)-P(1)	1.824(4)	N(1)-Os(3)	2.249(3)
C(12)-C(13)	1.381(5)	N(1)-H(1A)	0.9200
C(12)-H(12)	0.9500	N(1)-H(1B)	0.9200
C(13)-C(14)	1.383(6)	P(1)-Os(3)	2.3206(9)
C(13)-H(13)	0.9500	Os(1)-Os(2)	2.9028(2)
C(14)-C(15)	1.381(6)	Os(1)-Os(3)	2.9151(2)
C(14)-H(14)	0.9500	Os(2)-Os(3)	2.8626(2)

O(1)-C(1)-Os(1)	175.8(3)	O(5)-C(5)-Os(2)	178.7(4)
O(2)-C(2)-Os(1)	178.5(4)	O(6)-C(6)-Os(2)	176.3(3)
O(3)-C(3)-Os(1)	175.7(3)	O(7)-C(7)-Os(2)	175.5(3)
O(4)-C(4)-Os(1)	174.7(3)	O(8)-C(8)-Os(2)	176.9(3)

O(9)-C(9)-Os(3)	173.5(3)	C(17)-C(22)-P(1)	120.5(3)
O(10)-C(10)-Os(3)	174.6(3)	C(21)-C(22)-P(1)	120.5(3)
C(16)-C(11)-C(12)	119.1(3)	C(24)-C(23)-P(1)	107.7(3)
C(16)-C(11)-P(1)	122.9(3)	C(24)-C(23)-H(23A)	110.2
C(12)-C(11)-P(1)	117.8(3)	P(1)-C(23)-H(23A)	110.2
C(13)-C(12)-C(11)	120.5(4)	C(24)-C(23)-H(23B)	110.2
C(13)-C(12)-H(12)	119.7	P(1)-C(23)-H(23B)	110.2
C(11)-C(12)-H(12)	119.7	H(23A)-C(23)-H(23B)	108.5
C(12)-C(13)-C(14)	120.3(4)	N(1)-C(24)-C(23)	108.6(3)
C(12)-C(13)-H(13)	119.8	N(1)-C(24)-H(24A)	110.0
C(14)-C(13)-H(13)	119.8	C(23)-C(24)-H(24A)	110.0
C(15)-C(14)-C(13)	119.5(4)	N(1)-C(24)-H(24B)	110.0
C(15)-C(14)-H(14)	120.2	C(23)-C(24)-H(24B)	110.0
C(13)-C(14)-H(14)	120.2	H(24A)-C(24)-H(24B)	108.4
C(14)-C(15)-C(16)	120.6(4)	C(24)-N(1)-Os(3)	113.4(2)
C(14)-C(15)-H(15)	119.7	C(24)-N(1)-H(1A)	108.9
C(16)-C(15)-H(15)	119.7	Os(3)-N(1)-H(1A)	108.9
C(11)-C(16)-C(15)	119.9(4)	C(24)-N(1)-H(1B)	108.9
C(11)-C(16)-H(16)	120.1	Os(3)-N(1)-H(1B)	108.9
C(15)-C(16)-H(16)	120.1	H(1A)-N(1)-H(1B)	107.7
C(22)-C(17)-C(18)	120.3(4)	C(11)-P(1)-C(23)	105.94(17)
C(22)-C(17)-H(17)	119.8	C(11)-P(1)-C(22)	100.89(16)
C(18)-C(17)-H(17)	119.8	C(23)-P(1)-C(22)	106.48(17)
C(19)-C(18)-C(17)	120.1(4)	C(11)-P(1)-Os(3)	122.03(12)
C(19)-C(18)-H(18)	120.0	C(23)-P(1)-Os(3)	103.55(12)
C(17)-C(18)-H(18)	120.0	C(22)-P(1)-Os(3)	116.77(12)
C(18)-C(19)-C(20)	120.1(4)	C(4)-Os(1)-C(1)	89.90(16)
C(18)-C(19)-H(19)	119.9	C(4)-Os(1)-C(2)	99.47(16)
C(20)-C(19)-H(19)	119.9	C(1)-Os(1)-C(2)	100.42(16)
C(21)-C(20)-C(19)	120.2(4)	C(4)-Os(1)-C(3)	90.61(17)
C(21)-C(20)-H(20)	119.9	C(1)-Os(1)-C(3)	168.02(17)
C(19)-C(20)-H(20)	119.9	C(2)-Os(1)-C(3)	91.29(17)
C(20)-C(21)-C(22)	120.2(4)	C(4)-Os(1)-Os(2)	169.98(11)
C(20)-C(21)-H(21)	119.9	C(1)-Os(1)-Os(2)	87.36(11)
C(22)-C(21)-H(21)	119.9	C(2)-Os(1)-Os(2)	90.51(12)
C(17)-C(22)-C(21)	118.9(3)	C(3)-Os(1)-Os(2)	90.09(12)

C(4)-Os(1)-Os(3)	111.03(11)
C(1)-Os(1)-Os(3)	75.87(11)
C(2)-Os(1)-Os(3)	149.16(12)
C(3)-Os(1)-Os(3)	92.80(12)
Os(2)-Os(1)-Os(3)	58.949(5)
C(5)-Os(2)-C(7)	106.06(16)
C(5)-Os(2)-C(6)	90.88(16)
C(7)-Os(2)-C(6)	90.60(16)
C(5)-Os(2)-C(8)	91.64(16)
C(7)-Os(2)-C(8)	93.61(16)
C(6)-Os(2)-C(8)	174.31(15)
C(5)-Os(2)-Os(3)	88.69(11)
C(7)-Os(2)-Os(3)	164.83(11)
C(6)-Os(2)-Os(3)	92.74(11)
C(8)-Os(2)-Os(3)	82.22(11)
C(5)-Os(2)-Os(1)	149.25(11)
C(7)-Os(2)-Os(1)	104.67(11)
C(6)-Os(2)-Os(1)	87.61(11)
C(8)-Os(2)-Os(1)	87.62(11)
Os(3)-Os(2)-Os(1)	60.740(5)
C(10)-Os(3)-C(9)	89.04(17)
C(10)-Os(3)-N(1)	172.48(13)
C(9)-Os(3)-N(1)	87.27(14)
C(10)-Os(3)-P(1)	93.23(12)
C(9)-Os(3)-P(1)	98.52(11)
N(1)-Os(3)-P(1)	80.84(8)
C(10)-Os(3)-Os(2)	97.04(11)
C(9)-Os(3)-Os(2)	99.47(11)
N(1)-Os(3)-Os(2)	90.03(8)
P(1)-Os(3)-Os(2)	159.38(2)
C(10)-Os(3)-Os(1)	83.11(12)
C(9)-Os(3)-Os(1)	156.93(11)
N(1)-Os(3)-Os(1)	102.71(8)
P(1)-Os(3)-Os(1)	103.55(2)
Os(2)-Os(3)-Os(1)	60.311(5)

Symmetry transformations used to generate equivalent atoms:

Table **3.4.** Anisotropic displacement parameters ($Å^2 x\ 10^3$)for toste41. The anisotropic displacement factor exponent takes the form: $-2\pi^2[\ h^2 a^{*2} U^{11} + ... + 2\ h\ k\ a^*\ b^*\ U^{12}\ ]$

	U^{11}	U^{22}	U^{33}	U^{23}	U^{13}	U^{12}
C(1)	12(2)	23(2)	19(2)	-2(2)	6(2)	5(2)
C(2)	18(2)	22(2)	22(2)	1(2)	5(2)	-3(2)
C(3)	10(2)	25(2)	47(3)	3(2)	7(2)	3(2)
C(4)	16(2)	26(2)	18(2)	5(2)	3(2)	0(2)
C(5)	18(2)	22(2)	15(2)	-4(2)	2(2)	-2(2)
C(6)	16(2)	24(2)	14(2)	0(2)	6(2)	-2(2)
C(7)	13(2)	19(2)	20(2)	2(2)	2(2)	-3(2)
C(8)	22(2)	23(2)	11(2)	-1(2)	6(2)	0(2)
C(9)	18(2)	21(2)	14(2)	-2(2)	4(2)	-4(2)
C(10)	21(2)	22(2)	10(2)	-3(2)	1(2)	-2(2)
C(11)	11(2)	16(2)	11(2)	1(1)	1(1)	0(2)
C(12)	20(2)	19(2)	20(2)	0(2)	4(2)	-2(2)
C(13)	18(2)	25(2)	19(2)	7(2)	2(2)	-8(2)
C(14)	7(2)	36(2)	20(2)	9(2)	3(2)	4(2)
C(15)	20(2)	27(2)	26(2)	-2(2)	9(2)	7(2)
C(16)	21(2)	19(2)	18(2)	2(2)	4(2)	1(2)
C(17)	25(2)	25(2)	17(2)	2(2)	4(2)	6(2)

C(19)	19(2)	42(3)	24(2)	19(2)	2(2)	5(2)
C(20)	22(2)	45(3)	14(2)	5(2)	0(2)	-6(2)
C(21)	18(2)	30(2)	15(2)	0(2)	2(2)	0(2)
C(22)	10(2)	22(2)	13(2)	2(2)	4(2)	1(2)
C(23)	20(2)	15(2)	13(2)	-2(2)	4(2)	-3(2)
C(24)	17(2)	17(2)	15(2)	-2(2)	1(2)	-6(2)
N(1)	13(2)	17(2)	15(2)	0(1)	2(1)	1(1)
O(1)	25(2)	18(2)	37(2)	-6(1)	7(1)	0(1)
O(2)	34(2)	42(2)	24(2)	10(1)	-5(2)	-4(2)
O(3)	20(2)	23(2)	101(3)	-4(2)	5(2)	-5(1)
O(4)	17(2)	46(2)	28(2)	1(1)	10(1)	2(1)
O(5)	15(2)	39(2)	29(2)	-4(1)	3(1)	2(1)
O(6)	39(2)	18(2)	34(2)	-1(1)	13(1)	-8(1)
O(7)	26(2)	35(2)	16(2)	7(1)	-2(1)	-5(1)
O(8)	44(2)	19(2)	23(2)	-2(1)	14(1)	-4(1)
O(9)	20(2)	30(2)	29(2)	-1(1)	2(1)	10(1)
O(10)	42(2)	20(2)	18(2)	-1(1)	6(1)	-10(1)
P(1)	11(1)	13(1)	10(1)	-1(1)	2(1)	0(1)
Os(1)	9(1)	15(1)	15(1)	2(1)	3(1)	1(1)
Os(2)	11(1)	15(1)	10(1)	0(1)	2(1)	0(1)
Os(3)	10(1)	13(1)	9(1)	0(1)	2(1)	0(1)

Table **3.5.** Hydrogen coordinates (x 10^4) and isotropic displacement parameters ($Å^2$x 10^3) for compound **8**.

	x	y	z	U(eq)
H(12)	1982	6	3129	23
H(13)	-261	-87	3524	25
H(14)	-1147	1173	4014	25
H(15)	220	2530	4100	29
H(16)	2497	2630	3716	23
H(17)	5461	-526	3217	26
H(18)	6822	-1441	4047	35
H(19)	7679	-842	5081	34
H(20)	7102	655	5306	33
H(21)	5684	1563	4494	25
H(23A)	4240	2919	3085	19
H(23B)	5425	2589	3723	19
H(24A)	6745	3193	2921	20
H(24B)	7204	2152	3084	20
H(1A)	6589	2273	1987	18
H(1B)	5147	2770	1996	18

Bibliography

1. Schuster S. C. Next-generation sequencing transformation todays' biology. *Nature Methods* **2008**, 5(1), 16-18.

2. Kim, M. J.; Wanunu, M.W.; Bell, D. C.; Meller, A. Rapid Fabrication of uniformaly sized nanopores and nanopore arrays for parallel DNA analysis. *Adv. Mat.* **2006**, 18(23), 3149-3153.

3. Beer, M.; Moudrianakis, Determination of base sequence in nucleic acids with the electron microscope: visibility of a marker E. N. **1962** *Proc Natl Acad Sci U S A.* 48(3), 409-416.

4. Moudrianakis, E. N.; Beer, M. Determination of base sequence in nucleic acids with the electron microscope. II The reaction of a guanine-selective marker with the mononucleotides. *Biochim. Bioohys. Acta*, **1965**, 95, 23-39.

5. Fiskin, A. M.; Beer, M. Determination of base sequence in nucleic acid with the electron microscope. IV. Nucleoside complexes with certain metal ions. *Metal nucleoside complexes.* **1965**, 4(7), 1289-1294.

6. Moudrianakis, E. N.; Beer, M. Base sequence determination in nucleic acids with the electron microscope, III. Chemistry and microscopy of guanine-labeled DNA. *Biochemistry*, **1965**, 53, 564-571.

7. Beer, M. Stern, S. Carmalt, D. Mohlhenrich, K. H. Determination of base Sequence in nucleic acids with the electron microscope. V. The thymine-specific reactions of osmium tetroxide with deoxyribonucleic acid and its components. *Biochemistry*. **1966**, 5(7), 2283-2288.

8. Strothkamp, K. G.; Lippard, S. J. Platinum binds selectively to phophorothionate groups in mono- and polynucleotides: A general method for heavy metal staining of specific nucleotides. Proc. Natl. Acad. Sci. USA. **1976**, 73, 2536-2540.

9. Whiting, R. F.; Ottensmeyer, F. P. Heavy atoms in model compounds and nucleic Acid imaged by dark field transmission electron microscopy. *J Mol Biol.* **1972**, 67(2), 173-181.

10. Ottensmeyer, F. P. Molecular Structure Determination by High Resolution Electron Microscopy. *Ann. Rev. Biophys. Bioeng.* **1979,** 8, 129-144.

11. Andregg, W.; Andregg, M.; PCT Int. Appl. (**2009**). WO 2009046445 A1 20090409.

12. Payne, A. C.; Andregg, M.; Kemmish. K.; Hamalainen, M.; Bowell, C. Molecular Threading: Mechanical Extraction, Stretching and Placement of DNA Molecules from a Liquid-Air Interface. *PLoS ONE* **2013** 8(7).

13. Hayat, M. Principles and Techniques of Electron Microscopy: Biological Applications. 4th ed., Cambridge University Press, New York, **2000**.

14. Rosenberg, E.; Spada, F.; Sugden, K.; Martin, B.; Milone, L.; Gobetto, R.; Viale, A.; Fiedler, J. *J. Organometal. Chem* **2003**, 668, 51.

15. Rosenberg, E.; Spada, F.; Sugden, K.; Martin. B.; Gobetto, R.; Milone, L.; Viale, A. *J. Organomet. Chem.* **2004**, 689, 4729-4738.

16. Rosenberg, E.; Kumar, R. New methods for functionalizing biologically important molecules using triosmium metal clusters. *Dalton Trans.* **2012**, 41,714-722.

17. Heetebrij, R. J.; Talman, E. G.; Velzen, M. A. v.; Gijlswijk, R. P. M. v.; Snoeijers, S. S.; Schalk, M.; Wiegant, J.; Rijke, R. v. d.; Kirkhoven, R. M.; Raap, A. K.; Thane, H. J.; Reedijk, J.; Houthoff, H. J. Platinum(II)-based coordination compounds as nucleic acid labeling reagents: Synthesis, reactivity, and application in hybridization assays. *ChemBioChem,* **2003**, **3**, 573-583.

18. Erickson, H. P.; Beer, M. Electron microscopic study of base sequence in nucleic acids VI: preparation of RNA with marked GMP nucleotides. *Biochemistry* N. Y. **1967**, 6, 2694-2701.

19. Langmore, J. P.; Cozzarelli, N. R.; Crewe, A. V. A base specific single heavy atom stain for electron microscopy. *Proc. Electron Microscopy Soc. Am.* **1972**, 30, 184.

20. Frizell, J. A possible electron dense label for the use in the sequencing of DNA by electron microscopy. *J. Theor. Biol.* **1976**, 59, 241-242.

21. Kumar, R.; Rosenberg, E.; Feske, M. I.; DiPasquale, A. G. Relative rates of reaction of $Pt(en)Cl(NH_2R)^+$ with guanosine monophospahte as a function of amino group substituent: Toward efficient labeling of DNA for TEM imaging. *J. Organometal. Chem*. **2013**, 734, 53-60.

22. Priqueler, J. R. L.; Butler, I. S.; Rochon, F. D. An overview of ^{195}Pt nuclear magnetic resonance spectroscopy. Appl. Spectrosc. Rev. **2006**, 41, 185-226.

23. Materials Science and technology Group Oak Ridge National Laboratory P.O. Box 2008, Building 4515 1 Bethel Valley Road Oak Ridge, TN 37831-6071.

24. Hrovat, D. A.; Nordlander, E.; Richmond, M.G. DFT investigation of the mechanism of phosphine-thioether isomerization in the triosmium cluster $Os_3(CO)_{10}(Ph_2PCH_2CH_2SMe)$: Migratory preference for the formation of an edge-bridged thioether versus a phosphine moiety. *Organometallics,* **2012**, 31 6608-6613.

25. Deeming, A. J.; Hardcastle, K. I. Kabir, S. E. *J. Chem. Soc. Dalton Trans. Inorg. Chem*. (1988) 827-831.

26. Persson, R.; Monari, M.; Gobetto, R.; Russo, A.; Aime, S.; Calhorda, M. J.; Nordlander, E. Synthesis and characterization of triosmium clusters containing the bidentate ligand $Ph_2PCH_2CH_2SMe$: Detection of an isomerization reaction involving bridging and chelating ligand coordination modes. *Organometallics,* **2001**, 20 (20), 4150-4160.

27. Persson, R.; Stchedroff, M. J.; Uebersezig, B.; Gobetto, R.; Steed, J. W.; Prince, P. D.; Monari, M.; Nordlander, E. Synthesis, characterization, and novel fluxional mechanisms of triosmium clusters containing the highly flexible ligand $Ph_2PC_2H_4SC_2H_4SC_2H_4PPh_2$(PSSP). *Organometallics* **2010**, 29, 2223-2233.

28. Rosenberg, E.; Kabir, S. E.; Milone, L.; Gobetto, R.; Osella, D.; Hardcastle, K.I.; Hajela, S.; Wolf, E.; Moizeau, K.; Espisita, D. Comparative reactivity of triruthenium and triosmium μ_3-η^2-imidoyls. 1. Dynamics and reactions with carbon monoxide, phosphine, and isocyanide. *Organometallics,* **1997**, 16. 2665-2673.